' Traumatic brain injury is one of the most serious diseases that endanger human health. Sensitive and rapid detection method is a kind of powerful guarantee for the accurate and effective treatment of traumatic brain injury. In recent years' terahertz' THz' wave and Raman spectroscopy have broad application prospects in biomedical diagnosis and other fields due to their complementarity in technology. In this article' the researches of terahertz wave and Raman spectroscopy technology in traumatic brain injury detection were summarized in response to the needs and difficulties of traumatic brain injury diagnosis. Firstly' the development status of THz imaging and THz spectroscopy technology was introduced' and the applications of the two technologies in traumatic brain injury detection were also introduced' respectively. In addition' the principle and classification of Raman spectroscopy were summarized' and the research of Raman spectroscopy in the detection of traumatic brain injury tissues' body fluids' and biomarkers were discussed. Finally' the development trend of THz wave and Raman spectroscopy in the detection of traumatic brain injury was analyzed' which provides a new research idea for the application of THz wave and Raman spectroscopy in the rapid and accurate diagnosis of traumatic brain injury.

' terahertz wave' Raman spectroscopy' traumatic brain injury' terahertz time-domain spectroscopy' machine learning

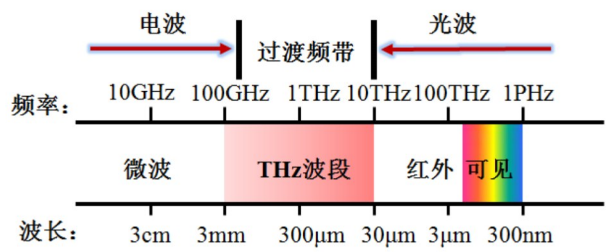

1'

Fig. 1' The frequency range of THz wave and its position in the electromagnetic spectrum

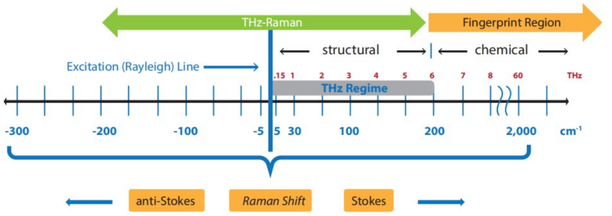

2’

Fig. 2’ The spectral range of Raman spectroscopy and the schematic diagram of the spectral information

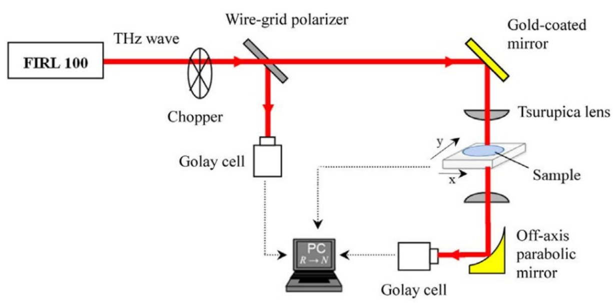

3’

Fig. 3’ Schematic of THz transmission imaging setup

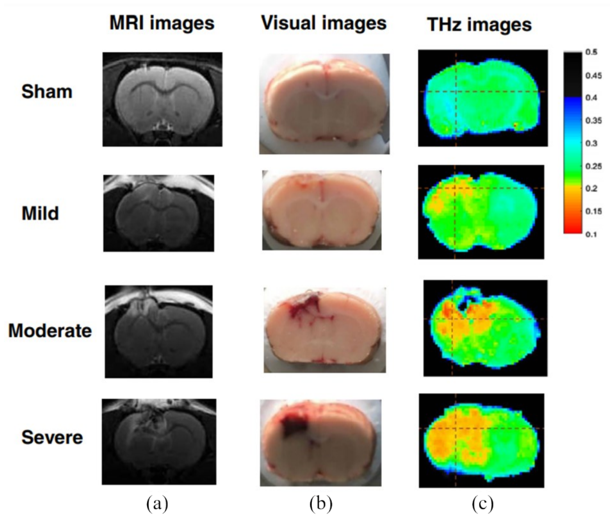

4 (a) (b) (c)

Fig. 4 (a) MRI images (b) visual images (c) THz images of fresh brain tissues without and with different degrees of traumatic brain injury

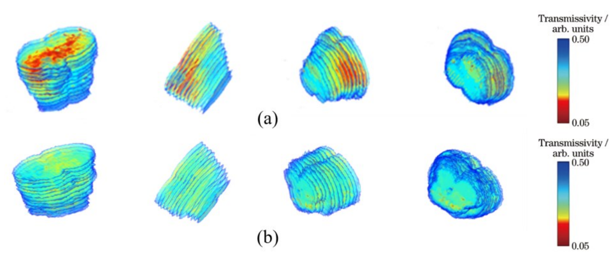

5 (a) (b)

Fig. 5 Three-dimensional model of (a) traumatic brain injury rat brain sample and (b) normal rat brain sample

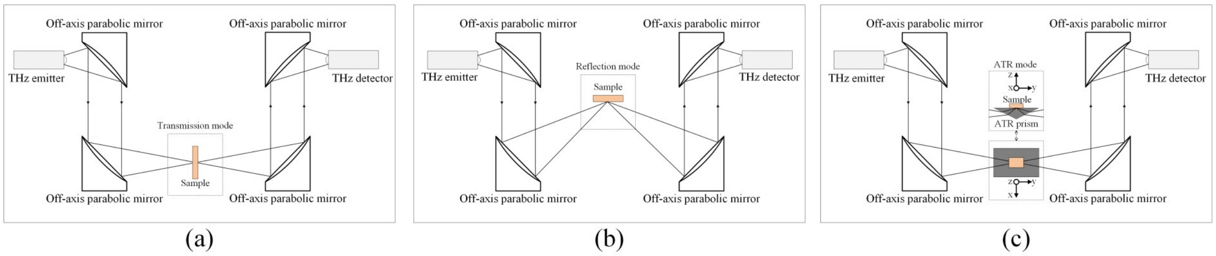

6 THz (a) THz (b) THz (c) THz-ATR

Fig. 6 Schematic of THz spectroscopy technology in (a) transmission mode, (b) reflection mode, and (c) ATR mode

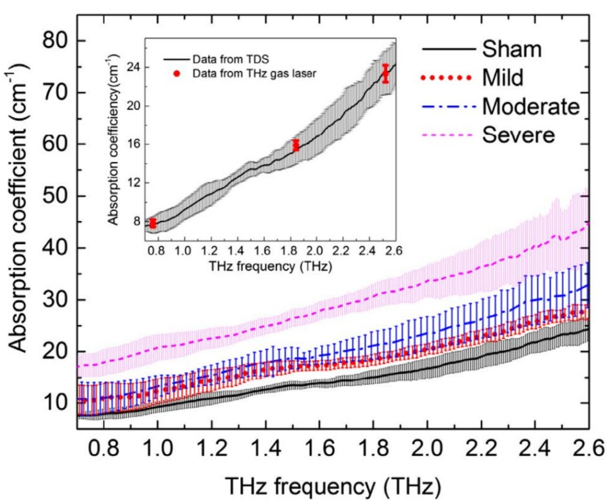

7

Fig. 7 THz absorption spectroscopy of paraffin-embedded brain tissue with different degrees of traumatic brain injury

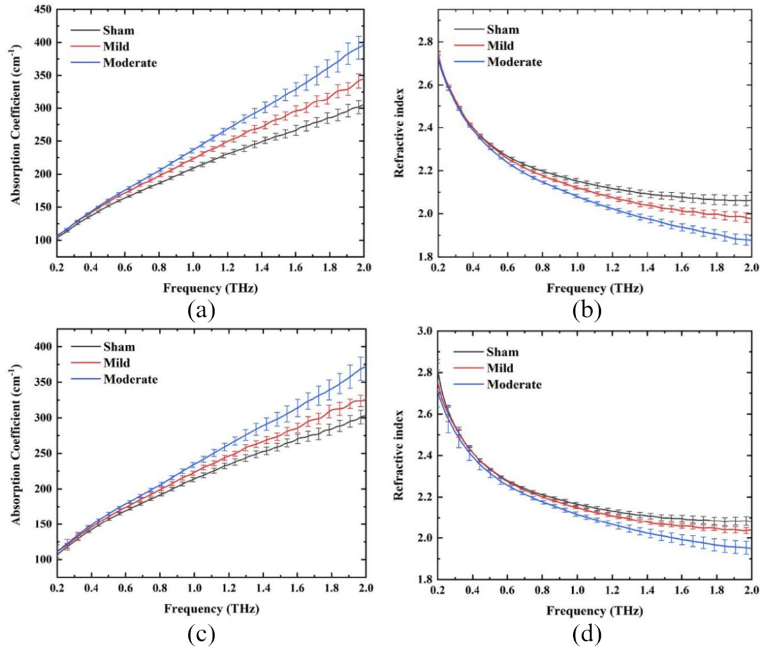

' 8' ' ' ' ' ' ' ' ' ' a ' ' ' ' ' ' ' ' ' ' ' ' " b ' ' ' ' ' ' ' ' ' ' ' c ' ' ' ' ' ' ' ' ' ' ' ' " d ' ' ' ' ' ' ' '

Fig. 8' ' a THz absorption coefficient spectroscopy' ' b THz refractive index spectroscopy of serum and' c THz absorption coefficient spectroscopy' ' d THz refractive index spectroscopy of cerebrospinal fluid

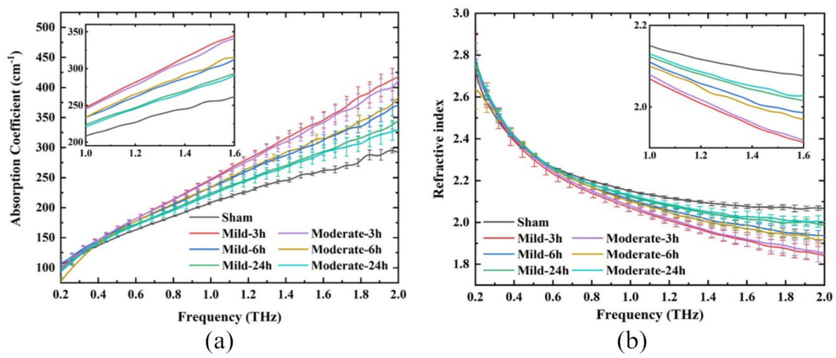

' 9' a ' ' ' ' ' ' ' ' ' ' ' ' " b ' ' ' ' ' ' ' ' '

Fig. 9' ' a THz absorption coefficient spectroscopy' ' b THz refractive index spectroscopy of total protein in hypothalamic of traumatic brain injury rats at different time

, , , , , , , , , , , , , , , , , ,

E E E E E E'

' ' E' ' ' ' ' ' ' ' ' ' ' ' ' EE

, , , , , , , EE' ' ' ' ' ' '

, , , , EE' ' ' ' ' ' ' ' ' ' ' ' '

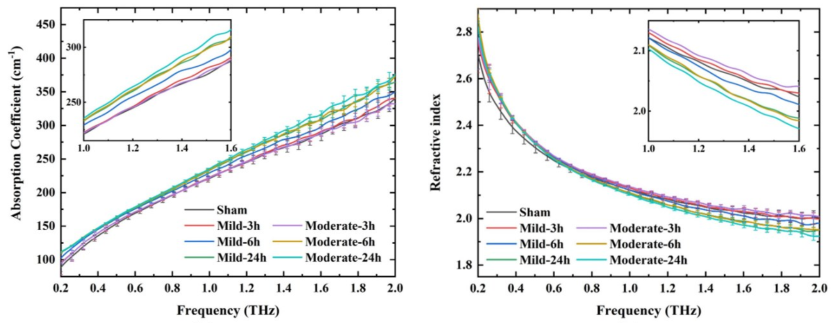

(a) (b)

10 a b

Fig. 10 a THz absorption coefficient spectroscopy b THz refractive index spectroscopy of total protein in hippocampal of traumatic brain injury rats at different time

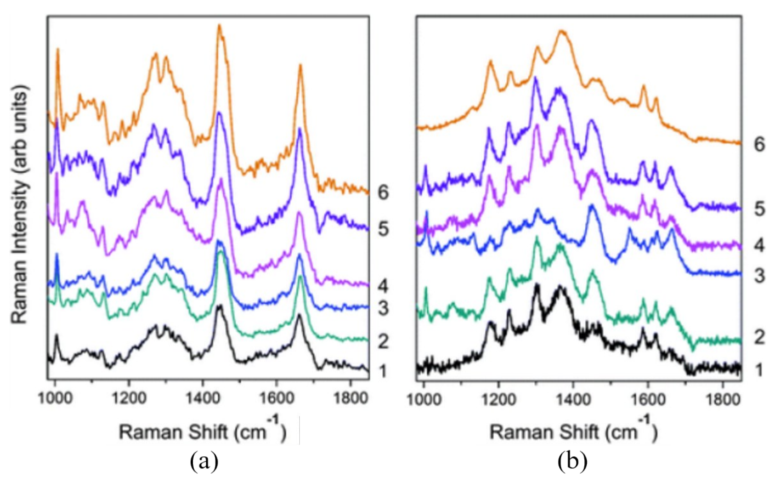

Fig. 11 Comparative Raman spectroscopy of healthy and injured mice brains. Raman spectra from the (a) control and (b) injured motor cortices demonstrate consistent Raman shifts following injury

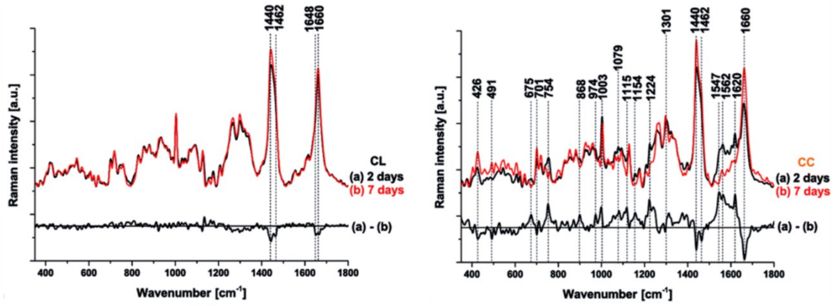

(a) (b)

12 a b 2 7

Fig. 12 Spectral differences of the average Raman spectral at 2 and 7 days after traumatic brain injury in (a) contralateral (CL) tissue and (b) contusion core (CC)

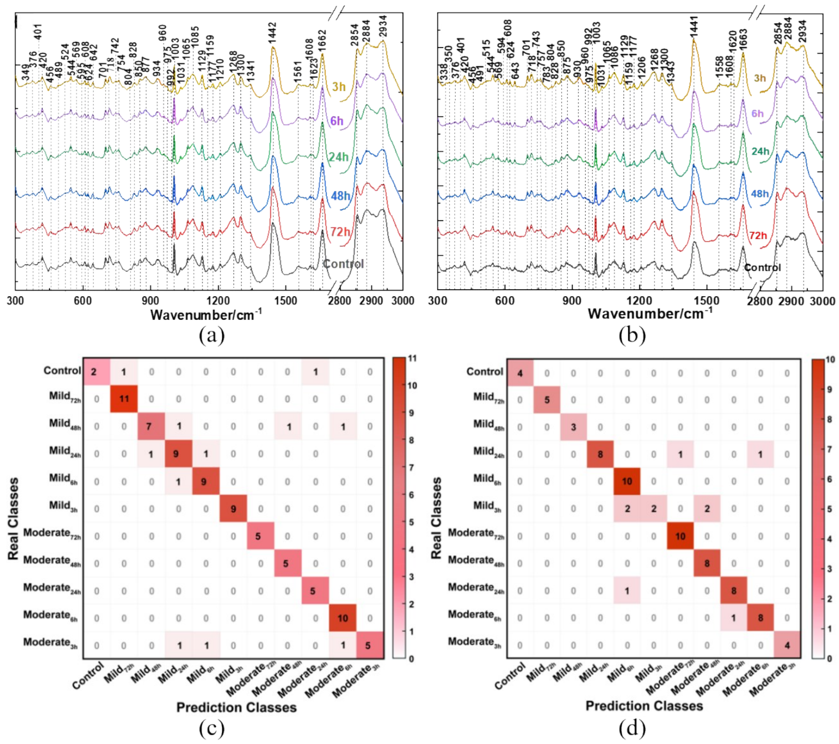

’ 13’ ’ ’ ’ ’ ’ ’ ’ ’ ’ ’ ’ ’ ’ ’ ’ ’ ’ ’ a ’ ’ ’ ’ ’ ’ ’ ’ ’ ’ ’ b ’ ’ ’ ’ ’ ’ ’ ’ ’ ’ ’ ’ ’ ’ ’ ’ ’ ’ 300~1 700 cm^{-1}’ ’ 2 800~3 000 cm^{-1}’ ’ ’ ’ ’ ’ ’ ’ ” c ’ ’ ’ ’ ’ ’ ’ ’ ’ ’ d ’ Linear Discriminant Analysis’ LDA’ ’ ’ ’ ’ ’ ’ ’ ’ ’ ’ ’ ’

Fig. 13’ ’ a The Raman spectra of hippocampus tissue’ ’ b hypothalamus tissue after mild bTBI’ the confusion matrix of LDA classifiers based on the Raman spectra of’ c hippocampus tissue’ and’ d hypothalamus tissue

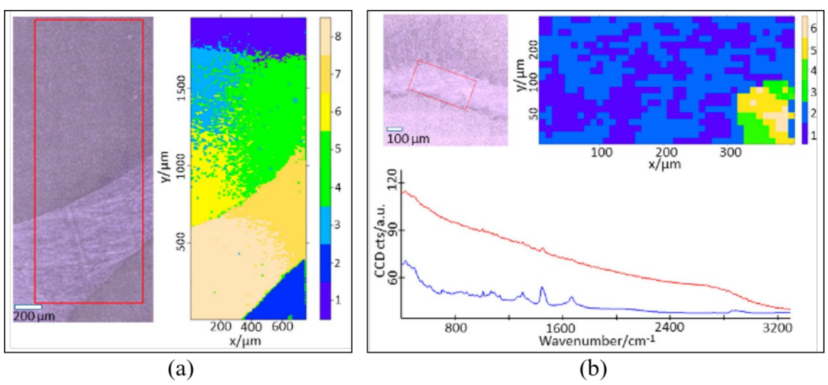

’ 14’ ’ ’ ’ ’ ’ ’ ’ ’ a ’ ” b ’ ’ ’

Fig. 14’ Light and Raman microscopy of the corpus callosum. ’ a light microscope image’ left panel’ and the corresponding Raman microscope image of the cortex and corpus callosum produced by hierarchical clustering analysis’ right panel’ . The area scanned with a Raman microscope is marked with a red rectangle. ’ b light microscope image’ top-left panel’ and the corresponding Raman microscope image of the corpus callosum with an abnormal region’ top-right panel’ . The mean Raman spectra of the corpus callosum’ blue color’ and the high intensity spectrum of the abnormal region’ red color’ are shown below’ bottom panel’

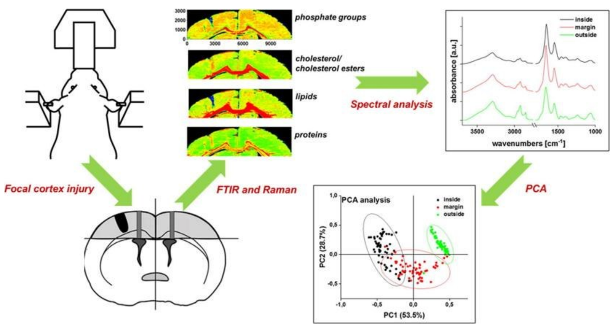

15

Fig. 15 Detection process and results of Fourier infrared microspectroscopy and Raman microspectroscopy

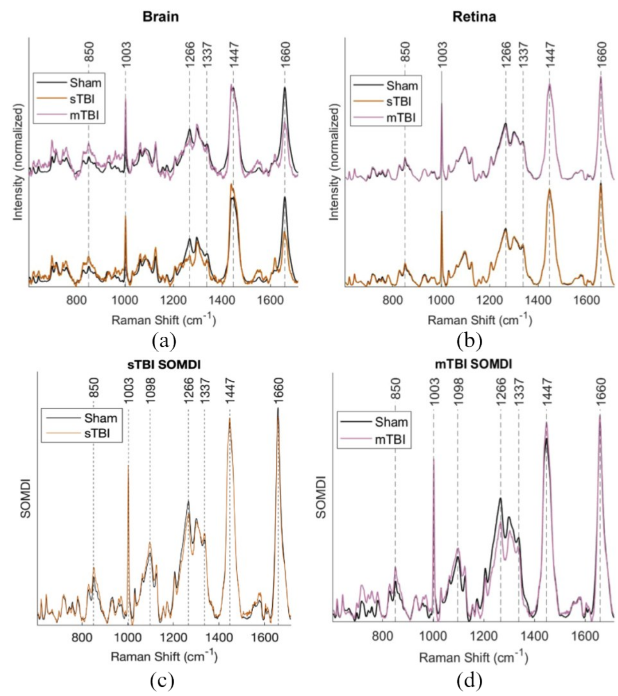

16 a b c d SOMs

Fig. 16 a Average Raman spectra collected in the contusion core for mTBI and sTBI compared to the sham group b average Raman spectra collected from flat mounted retina samples both eyes showing mTBI and sTBI compared to the sham group c Raman spectra of sTBI compared to the sham group of retina d Raman spectra of mTBI compared to the sham group of retina after feature extraction by SOMs

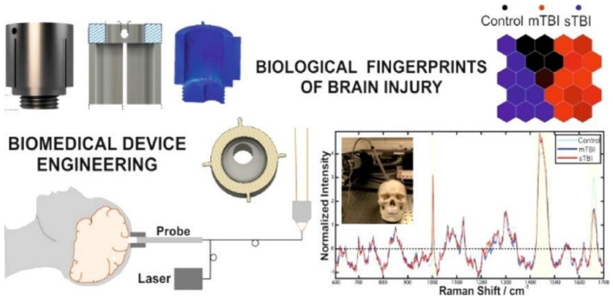

17

1 447/1 660 cm^{-1}

Fig. 17' Probe design' top-left panel' ' schematic diagram of the probe coupled to the optical fiber to acquire intracerebral Raman spectra' bottom-left panel' ' Raman images mapped using the characteristic peak 1 447/1 660 cm^{-1} peak ratio after control' moderate and severe traumatic brain injury' top-right panel' and spectral difference comparisons' bottom-right panel'

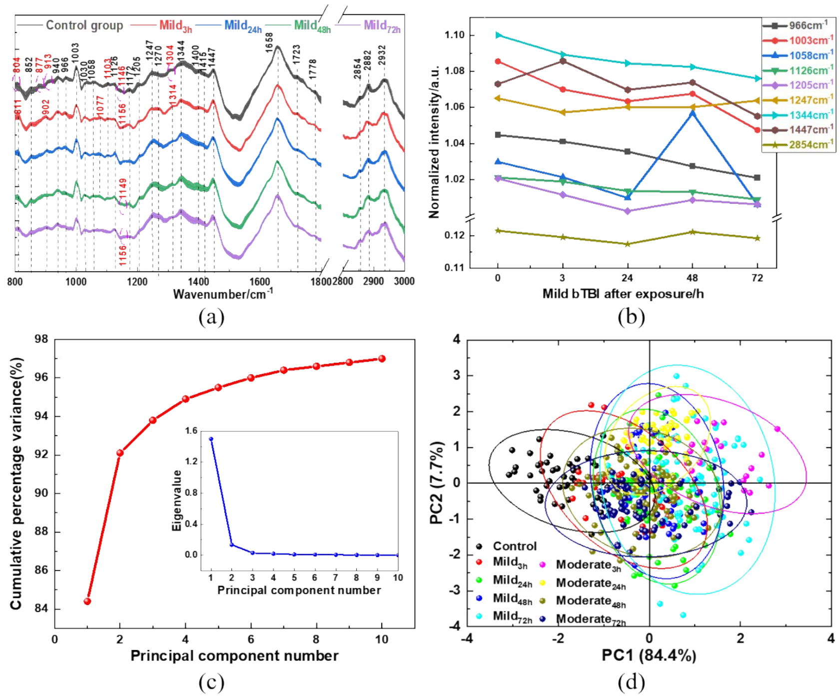

18 a bTBI b bTBI c 10 PC d PC

Fig. 18 a The Raman spectra of serum after mild bTBI b the Raman intensities change of mild bTBI at different time points the analysis results of PCA. c cumulative percentage of the variance of the first 10 PCs d scores of serum samples on the first two PCs